

# A dusty plasma model for vortex structure in Jupiter's atmosphere

Modhuchandra Laishram,<sup>1,\*</sup> Ping Zhu,<sup>1,2,3,†</sup> and Devendra Sharma<sup>4</sup>

<sup>1</sup>*CAS Key Laboratory of Geospace Environment and  
Department of Engineering and Applied Physics,*

*University of Science and Technology of China, Hefei 230026, China*

<sup>2</sup>*KTX Laboratory and Department of Engineering and Applied Physics,  
University of Science and Technology of China, Hefei 230026, China*

<sup>3</sup>*Department of Engineering Physics,*

*University of Wisconsin-Madison, Madison, Wisconsin 53706, USA*

<sup>4</sup>*Institute for Plasma Research, HBNI, Gujarat, India, 382428*

(Dated: November 26, 2018)

## Abstract

Structural changes of self-organized vortices in Jupiter's atmosphere such as Great Red Spot (GRS) and White Ovals are demonstrated using an electrostatically bounded charged dust cloud in an unbounded streaming plasma as the prototype for various driven-dissipative complex flow systems in nature. Using a 2D hydrodynamic model, the steady state flow solutions are obtained for the volumetrically driven dust cloud in a bounded domain of aspect-ratio of 1.5 relevant to the current size of GRS and a driving sheared ion flow similar to the part of zonal jets streaming through the GRS. These nonlinear solutions reveal many similar characteristic features between the steadily driven dust circulation in laboratory experiments and the vortices in Jupiter's atmosphere. Starting from the continuous structural changes, the persistence of high-speed collar ring around the quiescent interior of uniform vorticity of GRS and White Ovals are interpreted as a consequence of changes in internal properties related to kinematic viscosity rather than the driving fields. This analysis also sheds light on the roles of driving field, boundaries, and dynamical parameters regime in determining the characteristic size, the strength, the circulating direction, and the drift of the vortices in Jupiter's atmosphere and other relevant driven-dissipative flow systems in nature.

---

\* modhu@ustc.edu.cn

† pzhu@ustc.edu.cn

Jupiter is the largest planet in solar system whose atmosphere supports all kinds of dynamics starting from small-scale instabilities and turbulence up to large-scale steady zonal jets and colorful vortices [1–3]. The most distinctive feature of Jupiter’s atmosphere is its banded structure (Zones and Belts correlated with the sheared zonal jets) and immense vortices such as Great Red Spot (GRS) and White Ovals [4–7]. The GRS is a giant, long-lived, anti-cyclonic cloud vortex of the size  $14.1^\circ$  longitude by  $9.4^\circ$  latitude (where  $1^\circ = 1160 \text{ km}$ ), situated at central latitude  $22.3^\circ S$  of the Jupiter’s atmosphere [8], whereas the White Ovals are relatively small vortices observed at latitude  $33.8^\circ S$ ,  $41.8^\circ S$ , and  $19.0^\circ N$  [3, 5–7]. Both GRS and White Ovals have quiescent core region of uniform vorticity surrounded by collar rings of high velocity that dissociate the core region from the surrounding weak flows [3, 9]. Various spacecraft measurements have reported that GRS was first observed as a long pale hollow up to 1850s, then it became dusky elliptical rings up to 1870. Furthermore, it has been shrinking in size and accelerating in internal circulation ever since the late 1800s, while the streaming zonal jets have been globally stable around the GRS and White Ovals as shown in Fig. 1 [4, 10, 11].

Recently, NASA’s spacecraft (JUNO-2018) has once again confirmed most of the earlier observed characteristics of Jupiter’s atmosphere, such as the internal rotating period of GRS is decreasing, the giant vortex is shrinking with rate  $0.19^\circ/\text{year}$  along latitude,  $0.048^\circ/\text{year}$  along longitude, the overall structure is turning more circular with a negligible change in the streaming zonal jets [4, 8]. However, many puzzles over the physical interpretation of Jupiter’s vortices remain unsolved even after many years of observations and analysis, including the driving mechanism, the horizontal drift of GRS, the continuous structural change, the presence of high-speed collar rings around the quiescent interior, the long-life persistence of the vortices, and the actual three-dimensional structure, among others [3, 5, 10, 11]. There are various single fluid models using the concept of potential vorticity that interpret the vortices as Rossby soliton or turbulent inverse cascade driven by Coriolis force of the Jupiter [2, 12]. However, it has many criticisms regarding the flow profiles, the continuous structural changes, and the horizontal drift velocity among many others [12, 13]. Further, there are proposals that both the streaming zonal jets and the vortices of Jupiter’s atmosphere are driven by the moist convection or the thermal convective instability from the deep interior, and the energy from small-scale eddies, but these are doubtful to be the main drivers of such giant vortices [14]. The actual mechanisms for the dynamics and peculiar

characteristics features of these vortices still remain unclear.

On the other side, the GRS and White Ovals are reported as driven-dissipative complex flow systems consisting of multiple species  $NH_3$ ,  $CH_4$ ,  $Ar$ ,  $NH_4SH$ , and  $H_2O$ -ice in dynamic equilibrium with the zonal jets and other in-out forcing factors such as Coriolis effect and thermo-convection moist [2, 15, 16]. Moreover, the size, the strength, and the direction of vortices in Jupiter's banded structure are strongly correlated with the position and shear strength of the streaming jets, which we believe to be the main driver for the Jupiter's vortices [3, 5, 8, 10]. And surprisingly, we find the characteristics of GRS and White Ovals are found too much resemble that of bounded dust cloud circulation in an unbounded streaming plasma [17–20]. For example, in one of recent laboratory experiments (please see fig. S1 in the Supplementary Materials) and its theoretical formulation at a higher flow velocity regime [17, 20], we have observed compelling nonlinear features of dust-vortex dynamics having a nearly uniform vorticity in the core region surrounded by highly shear layers, and many regions of highly accelerating and deceleration in velocity field (please see fig. S2 in the Supplementary Materials), which are very similar to the flow characteristics of the Jupiter's GRS and White Ovals [17, 20]. These common characteristics and physics shared by both systems motivates us to adopt the dynamics of the confined dust cloud in the streaming plasma as a prototype for studying various characteristics of GRS and White Ovals. Further, it has been well known that GRS has thin, but wide upper layers along with a relatively steady vertical stratified deeper layers inside, which does not affect much on the dynamics of upper layers [2, 3, 7]. Therefore, this structure allows us to approximate the surface dynamics independent of the deep interior, which is closely similar to the dynamics within the 2D cross-section of the electrostatically confined dust cloud in the streaming plasma.

Considering the resemblance of dynamics of GRS and White Ovals to that of the bounded dust cloud in the streaming plasma which follows the incompressible and isothermal conditions, the dynamics of both systems in a 2D  $XY$ -plane, though vastly different in appearance, may be modeled using the modified Navier-Stokes equations in terms of the stream function  $\psi\hat{z}$  and the flow vorticity  $\omega\hat{z}$  as follows [20–22],

$$\nabla^2\psi = \omega, \tag{1}$$

$$\frac{\partial\omega}{\partial t} + (\mathbf{u} \cdot \nabla)\omega = \mu\nabla^2\omega - \xi(\omega - \omega_s) - \nu\omega. \tag{2}$$

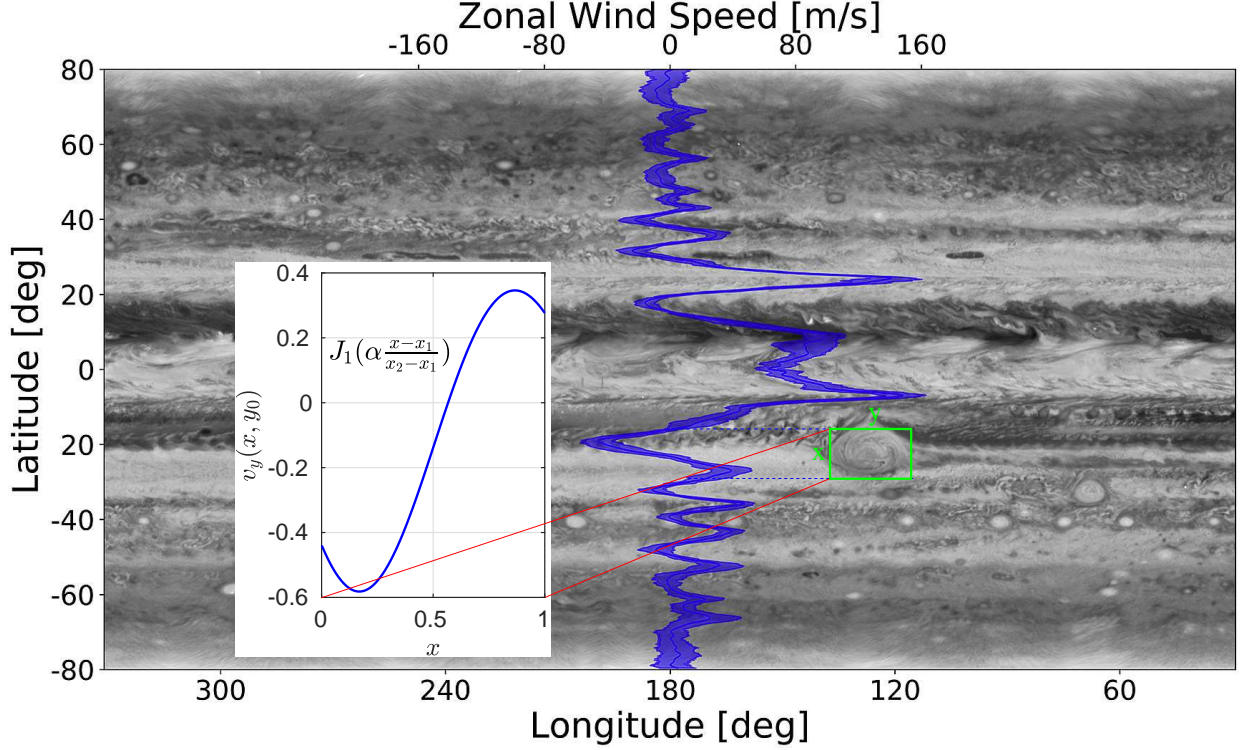


FIG. 1. Jupiter’s zonal jets profile (inset) taken from the region in green box in the Hubble Space Telescope (HST) image of Jupiter. Reproduced with permission from *Planet. Space Sci.* **155**, 2-11 (2018) [4].

Here,  $\hat{z}$  is unit vector normal to the  $XY$ -plane,  $\mathbf{u}$  is the dust flow velocity,  $\omega_s$  is the collective vorticity source from the sheared streaming background plasma. And the dynamic regime is determined by system parameters  $\mu$ ,  $\xi$ , and  $\nu$  [23–25]. For a laboratory glow discharge argon plasma, a typical set of parameters are  $n \simeq 10^9 \text{ cm}^{-3}$ ,  $T_e \simeq 3eV$ ,  $T_i \simeq 1eV$ , with system size  $L_x \sim 10 \text{ cm}$ , and ions shear flow strength  $U_0$  equivalent to the fraction of ion acoustic velocity  $c_s = \sqrt{T_e/m_i}$ , the value of parameters are  $\xi \sim 10^{-4} U_0/L_x$ ,  $\nu \sim 10^{-3} U_0/L_x$ , and  $\mu \sim 1 \times 10^{-4} U_0 L_x$  respectively [20, 25, 26]. In the case of Jupiter’s vortices,  $\omega$  and  $\psi$  are the relative vorticity and corresponding stream function of the clouds driven by shear zonal jets of vorticity  $\omega_s$ . And  $\mu$  takes the role of kinematic viscosity of the driven clouds,  $\xi$  is the interactions coefficients of the clouds with the streaming zonal jets, and  $\nu$  is the interactions coefficients with the stationary background which maintain the steady flows. The corresponding absolute vorticity  $\omega_{abs}$  in presence of stretching vorticity  $\omega_{st}$  (3D effects) and Coriolis force at the planetographic latitude  $\phi$  and angular velocity  $\Omega$  of the planet is

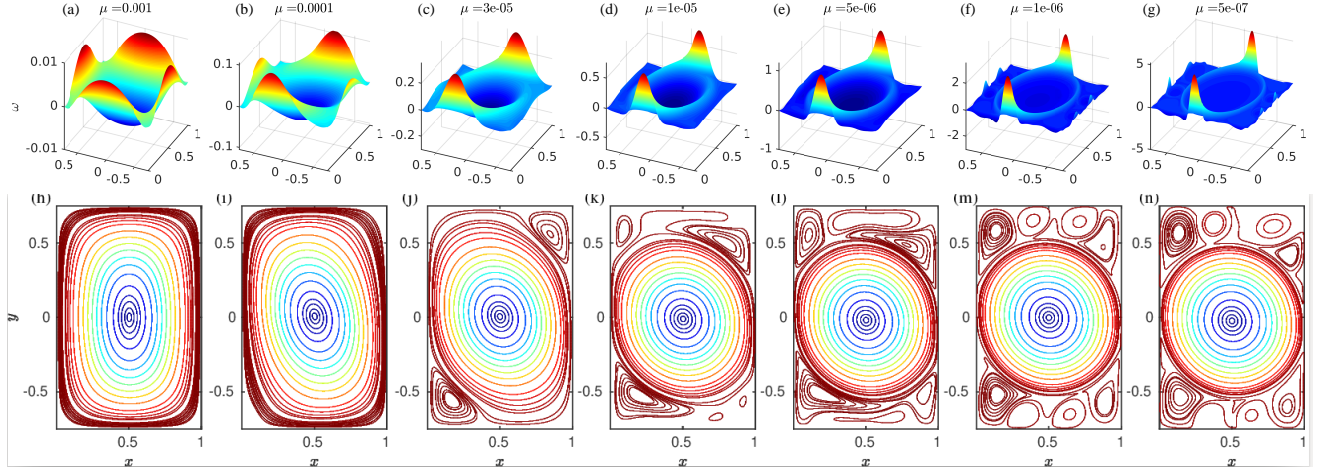


FIG. 2. Structural changes in steady-state dust vorticity (a) to (g), and corresponding streamline pattern (h) to (n), for a wide range of parameter  $\mu$  from  $1 \times 10^{-3} U_0 L_x$  to  $8 \times 10^{-7} U_0 L_x$  and fixed other system parameters.

$\omega_{abs} = \omega + \omega_{st} + 2\Omega \sin(\phi)$  [2]. However, the present analysis emphasizes only on the  $\omega$  and  $\psi$  of the steady flow because the effect of stretching vorticity and Coriolis force are only to change the strength of absolute vorticity uniformly.

The steady-state solutions of the above set of equations (1)-(2) are obtained using proper boundary conditions and vorticity sources relevant to the bounded Jupiter's vortices [10, 11, 22, 25]. Real confined systems allow having an arbitrarily shaped cross-section determined by the confining potential. However, for simplicity, we select a rectangular domain of aspect-ratio  $L_y/L_x = 1.5$  relevant to the current size of the GRS displayed in Fig. 1 [4, 10]. Within the domain, the GRS is a partially bounded quasi-steady circulation in presence of the stable streaming zonal jets, whose profile has a westward peak at  $19.5^\circ S$  and a relatively weak eastward peak at  $26.5^\circ S$ . This may be the reason for the existence of horizontal drift of the GRS towards the West [4, 8, 10]. Thus, the main driver  $\omega_s$ , i.e., the streaming ions in our model is considered to take a profile similar to a portion of the sheared zonal jets streaming through the GRS as highlighted (by blue color) in the Fig. 1.

Now, a series of the steady-state dust flow structure in term of the vorticity( $\omega$ ) and corresponding streamline patterns (i.e., contours of  $\psi$ ) in the rectangular  $XY$ -plane are displayed in Fig. 2, for a wide range of kinematic viscosity  $\mu$  and fixed other dependence on  $\omega_s$ ,  $\xi$ , and  $\nu$ . In the case of highly viscous regime  $\mu \sim 10^{-3} U_0 L_x$ , the flow vorticity along boundary is relatively weak, symmetric, and uniformly diffusive throughout the whole

domain as shown in Fig. 2(a). And the corresponding streamline pattern is the rectangular circulations following the geometry of confined domain as shown in Fig. 2(h). Then, decrease in  $\mu$  leads the vorticity profile to strengthen and become asymmetric as shown in Fig. 2(b) – (c). The corresponding streamline in Fig. 2(i) – (j) turn into elliptical circulations that can retain more angular velocity ( $\approx 2\omega$ ) without a significant change in the angular momentum of the system. Thus, the dynamical changes with the decrease in  $\mu$  give a new state of the flow that retains more momentum or energy, and as a consequence, the new flow structure starts to form because of the dynamical regime rather than the geometry of bounded domain. Thus, for a further decrease in  $\mu$ , the asymmetry in vorticity profile gets enhanced such that highly sheared layers develop near the boundary along the driving ions and flatten near the boundary across the driver as shown in Fig. 2(d) – (e). The relative increase in convective transport enables the vorticity near the boundaries to convect along the streamlines and then dissipate to the background instead of diffuse directly towards the interior region. Therefore, the corresponding streamline patterns in Fig. 2(k) – (l) become more circular and turn into a new self-organized state with a circular core region surrounded by high-speed collar layers that dissociate the core from the surrounding regions filled with weak and elongated vortices. This qualitative change in vorticity or streamline patterns takes place through a critical parameter  $\mu^*$ , and this phenomenon is known as nonlinear structural bifurcation [20, 27]. Further, in the case of highly nonlinear regime  $\mu \leq 10^{-6}U_0L$ , the driven system retains more momentum and hence the vorticity along the collar layers and near the boundaries are strengthened, developing a flat uniform vorticity core region in the interior as shown in Fig. 2(f) – (g). The corresponding streamline patterns in Fig. 2(m) – (n), indicate that there is no significant change in the circular core region, however, the weak and elongated vortices near the boundaries also get strengthened and becomes more circular like the primary core vortex.

The structural changes in the vorticity and corresponding streamline patterns of the bounded dust flow are again demonstrated in terms of cross-section profiles of velocity  $u_x$  and  $u_y$  passing through the center of the circulation  $(x_0, y_0)$  as shown in Fig. 3(a) and (b). Here both  $u_x$  and  $u_y$  strengthen in amplitude with decreasing  $\mu$ . And along the transitions, the monotonic variation of  $u_x$  along  $y$ -direction near boundary turns oscillatory when the viscosity drops below the critical viscosity  $\mu^*$ , indicating the nonlinear structural bifurcation and the emergence of small-scale dynamics in the system. Further, with increasing

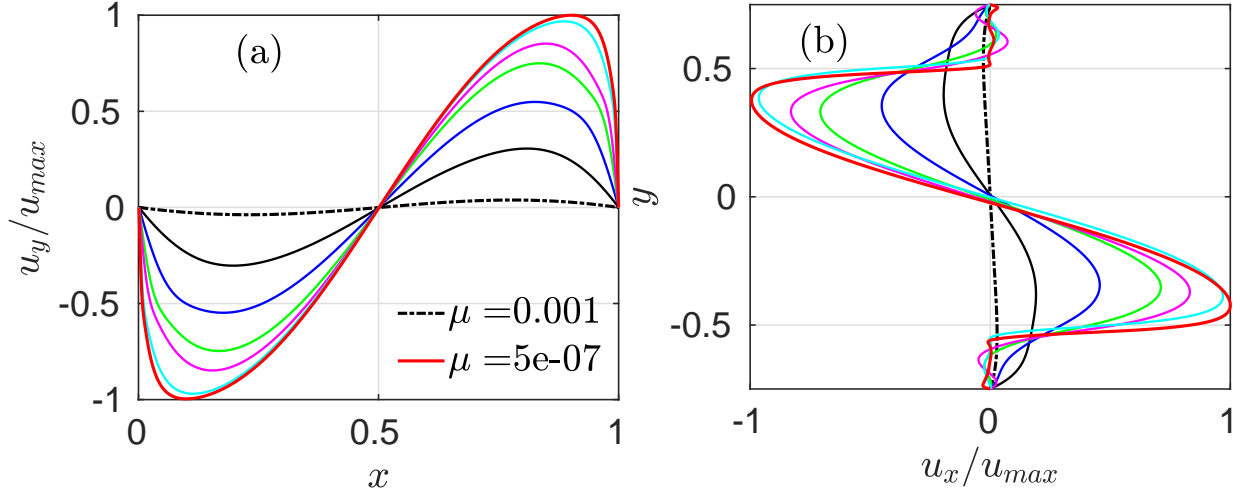


FIG. 3. Cross-section profiles of steady dust flow velocity (a)  $u_y/u_{max}$  and (b)  $u_x/u_{max}$  for the wide range of kinematic viscosity  $\mu$ .

nonlinearity, both  $u_x$  and  $u_y$  approach constant steady flow speeds with a single shear scale between two equidistant opposite peaks, denoting the emergence of the high-speed collar layers or virtual boundary (separatrix) which separates the circular core region of uniform vorticity away from the weak flows near boundaries. The characteristic size of the core region is determined by the dominant scale such as the smallest distance between two opposite boundaries or shear scale of the driving field [20, 25].

The series of steady flow structures of the bounded driven dust cloud with changing  $\mu$  in Fig. 2 sheds light on the similar phenomena of structural changes of GRS and White Ovals, which are turning more circular without changing the driver zonal jets [10, 28]. It indicates that the structural changes in vortices of the Jupiter's atmosphere are mainly due to a change in its internal properties related to the viscosity  $\mu$  rather than the changes in the drivers. Therefore, the driven vortex is accelerating, the circulation period is decreasing, and the structure becomes more circular without a significant change in the total angular momentum of the whole system. Further, the emergence of the self-organized state with a circular core region of uniform vorticity surrounded by high-speed collar layers is quite similar to the presence of quiescent interior and high-speed collar rings of GRSs and White Ovals [3, 9]. The primary core region of uniform vorticity displayed in the Fig. 2 and the corresponding velocity profile in Fig. 3(a) and (b) at highly nonlinear regimes satisfy the

Prandtl-Batchelor Theorem ( $\frac{\partial \omega}{\partial \psi} \approx 0$  means  $\mu \oint \nabla^2 u \cdot d\mathbf{l} \approx 0$ ) i.e., the core region is free from viscous dissipation (please see fig. S3 in the Supplementary Materials) [20, 29]. Once the fully circular structure of uniform vorticity emerges in any of the driven-dissipative systems, it persists or does not change its characteristics in a wide range of nonlinear regimes, whereas the surrounding weak vortices change accordingly. This is a possible explanation why the similar flow systems such as GRS and White Ovals have been persisting for a long time, even more than hundreds of years. It further gives the intuition that the quasi-steady circular vortices in the Jupiter's atmosphere may persist for a long life in future unless any dissipative mechanism is developed in the system. Furthermore, the shear nature of the dust velocity profile  $u_x$  and  $u_y$  at highly nonlinear regime displayed in Figs 3(a) and (b) is in close agreement with the observations in dusty plasma experiments [17] and that of the North-South and the East-West global velocity profile of White Ovals BA (please see fig. S4 in the Supplementary Materials) [6, 7].

Among the notable issues with this model, the scales of the dust dynamics are not identical to the real Jupiter's atmosphere and it can not able to interpret the turbulence behaviors at the center of the GRS which are expected to be 3D-effects from the interior [14]. However, vortices in the whole banded structure of Jupiter atmosphere have different size, strength, and direction depending on the shear nature of the zonal jets. These phenomena support the argument that the streaming zonal jets are the dominant driver of the vortices even though the vortices have additional effects of Coriolis force and 3D-effects which may actually strengthen or weaken the absolute vorticity. In short, this work has demonstrated various observed characteristic features of Jupiter's vortices are the consequence of changes in internal properties related to kinematic viscosity rather than the driving fields.

## I. ACKNOWLEDGMENTS

Author L. Modhuchandra acknowledges late Prof. P. K. Kaw, Institute for Plasma Research, India, for the invaluable supports and encouragements. The research was supported by the State Administration of Foreign Experts Affairs - Foreign Talented Youth Introduction Plan Grant No. WQ2017ZGKX065, the National Magnetic Confinement Fusion Program of China under Grant Nos. 2014GB124002 and 2015GB101004. Author P. Zhu



also acknowledges the support from U.S. DOE grant Nos. DE-FG02-86ER53218 and DE-FC02-08ER54975. The work used the resources of Supercomputing Center of University of Science and Technology of China.

---

- [1] P. S. Marcus, *Nature (London)* **331**, 693 (1988).
- [2] P. S. Marcus, *Annu. Rev. Astron. Astrophys.* **31**, 523 (1993).
- [3] A. R. Vasavada, A. P. Ingersoll, D. Banfield, M. Bell, P. J. Gierasch, M. J. Belton, G. S. Orton, K. P. Klaasen, E. DeJong, H. Breneman, T. J. Jones, J. M. Kaufman, K. P. Magee, and D. A. Senske, *Icarus* **135**, 265 (1998).
- [4] P. E. Johnson, R. Morales-Juberas, A. Simon, P. Gaulme, M. H. Wong, and R. G. Cosentino, *Planet. Space Sci.* (2018).
- [5] A. A. Simon, M. H. Wong, J. H. Rogers, G. S. Orton, I. de Pater, X. Asay-Davis, R. W. Carlson, and P. S. Marcus, *Astrophys J.* **797**, L31 (2014).
- [6] D. S. Choi, A. P. Showman, and A. R. Vasavada, *Icarus* **207**, 359 (2010).
- [7] P. S. Marcus and S. Shetty, *Phil. Trans. R. Soc. A* **369**, 771 (2011).
- [8] A. A. Simon, F. Tabataba-Vakili, R. Cosentino, R. F. Beebe, M. H. Wong, and G. S. Orton, *The Astronomical Journal* **155**, 151 (2018).
- [9] J. L. Mitchell, R. F. Beebe, A. P. Ingersoll, and G. W. Garneau, *J. Geophys. Res.* **86**, 8751 (1981).
- [10] J. H. Rogers, *J. Br. Astron. Assoc.* **118** (2008).
- [11] A. A. Simon-Miller, P. J. Gierasch, R. F. Beebe, B. Conrath, F. Flasar, and R. K. Achterberg, *Icarus* **158**, 249 (2002).
- [12] P. S. Marcus and C. Lee, *Quasigeostrophic flow Chaos* **4**, 269 (1994).
- [13] T. E. Dowling and A. P. Ingersoll, *J. Atmos. Sci.* **46**, 3256 (1989).
- [14] A. P. Ingersoll, P. J. Gierasch, D. Banfield, A. R. Vasavada, and G. I. Team, *Nature* **403**, 630 (2000).
- [15] M. J. Loeffler, R. L. Hudson, N. J. Chanover, and A. A. Simon, *Icarus* **271**, 265 (2016).
- [16] S. Weidenschilling and J. Lewis, *Icarus* **20**, 465 (1973).
- [17] M. Kaur, S. Bose, P. K. Chattopadhyay, D. Sharma, J. Ghosh, Y. C. Saxena, and E. T. Jr., *Phys. Plasmas* **22**, 093702 (2015).

- [18] M. Kaur, S. Bose, P. K. Chattopadhyay, D. Sharma, J. Ghosh, and Y. C. Saxena, *Phys. Plasmas* **22**, 033703 (2015).
- [19] A. P. Nefedov, G. E. Morfill, V. E. Fortov, H. M. Thomas, H. Rothermel, T. Hagl, A. V. Ivlev, M. Zuzic, B. A. Klumov, A. M. Lipaev, V. I. Molotkov, O. F. Petrov, Y. P. Gidzenko, S. K. Krikalev, W. Shepherd, A. I. Ivanov, M. Roth, H. Binnenbruck, J. A. Goree, and Y. P. Semenov, *New J. Phys.* **5**, 33 (2003).
- [20] M. Laishram, D. Sharma, P. K. Chattopdhyay, and P. K. Kaw, *Phys. Rev. E* **95**, 033204 (2017).
- [21] L. Landau and E. Lifshitz, *Fluid Mechanics*, v. 6 (Elsevier Science, 2013).
- [22] M. Laishram and P. Zhu, *Physics of Plasmas* **25**, 103701 (2018).
- [23] M. S. Barnes, J. H. Keller, J. C. Forster, J. A. O'Neill, and D. K. Coultas, *Phys. Rev. Lett.* **68**, 313 (1992).
- [24] M. Laishram, D. Sharma, and P. K. Kaw, *Phys. Plasmas* **21**, 073703 (2014).
- [25] M. Laishram, D. Sharma, and P. K. Kaw, *Phys. Rev. E* **91**, 063110 (2015).
- [26] G. Salin and J.-M. Caillol, *Phys. Rev. Lett.* **88**, 065002 (2002).
- [27] M. Ghil, J.-G. Liu, C. Wang, and S. Wang, *Physica D* **197**, 149 (2004).
- [28] I. Barrado, H. Rojas, Sanchez-Lavega, D. Colas, Peach, and IOPW-Team, *Astron. and Astrophys* **554**, A74 (2013).
- [29] G. K. Batchelor, *J. Fluid Mech.* **1**, 177190 (1956).